Biophysical Chemistry, 39 (1991) 91–106
Elsevier

BIOCHE 01529

Binding and diffusion kinetics of the interaction of a hydrophobic potential-sensitive dye with lipid vesicles

R.J. Clarke

School of Chemical Sciences, University of East Anglia, Norwich NR4 7TJ, U.K.

Received 27 March 1990
Revised manuscript received 2 August 1990
Accepted 7 August 1990

Dye binding; Lipid vesicle; Fluorescence quenching; Membrane potential; Diffusion; Kinetics

The interaction of the dye oxonol V with unilamellar dioleoylphosphatidylcholine vesicles has previously been investigated using a fluorescence stopped-flow technique. It has been found that the most suitable mathematical description of the equilibrium and kinetic data is obtained by assuming the presence of saturable dye binding sites in both monolayers of the vesicle membrane and a potential-dependent diffusion across the membrane interior between these two classes of sites. A kinetic model is presented which takes into account the degree of saturation of the binding sites, the degree of fluorescence quenching within the membrane, and the production of an electrical potential gradient across the membrane interior by the binding of the negatively charged dye. The model successfully predicts the time course of the fluorescence change due to binding and diffusion over the complete range of dye and vesicle concentrations as well as the fluorescence response of the dye to changing membrane potential.

1. Introduction

Potential-sensitive dyes have been widely used in recent times for measuring membrane potentials of cells, cell organelles and membrane vesicles [1–5]. A change in membrane potential results in an alteration in the dye fluorescence or absorption signal. From this dye response the membrane potential can be determined, assuming that the dye response has previously been calibrated at known membrane potentials. Although the application of potential-sensitive dyes in biochemical research may not necessarily require a complete understanding of the mechanism of the dyes' response, knowledge of their mechanisms may yield information useful in designing better probe molecules. In themselves they are also interesting in that they provide a model system for studying the interaction of small hydrophobic species with lipid membranes. Of further practical importance is the possibility of selectively staining cancerous cells and thus using dyes as photoactive anticancer therapeutic agents [6–8].

Oxonol dyes, such as oxonol V and VI (see fig. 1), have been widely used as potential-sensitive dyes in membrane experiments [9]. They have a pK_a near 4.2 [10] and are thus anionic at physiological pH values, but the charge is delocalized over the molecule, so that they are still membrane permeable. Because of their hydrophobicity they bind strongly to lipid membranes and consequent

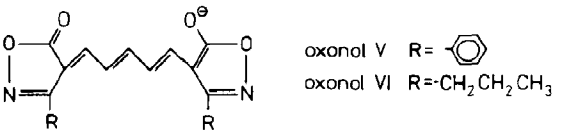

Fig. 1. Structures of oxonol V and VI.

Correspondence (present) address: R.J. Clarke, Fritz-Haber-Institut der Max-Planck-Gesellschaft, Faradayweg 4-6, D W-1000 Berlin 33, Germany.

changes in their absorbance and fluorescence spectra are observed.

In a previous paper [9], stopped-flow kinetic data were presented for the interaction of oxonols V and VI with lipid vesicles and their response to changing membrane potential. It was found that the data for the binding step could be adequately described under conditions of excess vesicle assuming a simple model involving consecutive association steps of dye to vesicle, and rate constants for binding and dissociation were determined. At high dye/lipid concentration ratios, however, this simple model was found to be no longer adequate to explain all the experimental observations. For example, at low dye/lipid concentration ratios an increase in fluorescence is observed, however, as one proceeds to higher dye/lipid concentration ratios a reversal of the sign of the fluorescence change occurs due to quenching processes. Certain aspects of the kinetics of diffusion across the membrane could also previously only be qualitatively described. For example, it was found that the rate of diffusion of oxonol V across the membrane was sensitive to the magnitude of the membrane potential, whereas in the case of oxonol VI the diffusion rate appeared to be independent of the membrane potential.

In the present paper, the kinetic theory is significantly extended to include both binding and diffusion steps for the complete range of dye and vesicle concentrations. Equilibrium data are also presented which provide information necessary for the simulation of the kinetic traces. The extended kinetic model predicts the time course of the fluorescence change due to binding and diffusion as well as the response to a change in membrane potential.

2. Materials and methods

2.1. Materials

Dioleoylphosphatidylcholine was obtained from Avanti Polar Lipids (Birmingham, AL, U.S.A.); oxonol V (bis(3-phenyl-5-oxoisooxazol-4-yl)pentamethine oxonol) was from Molecular Probes (Junction City, OR, U.S.A.). The phospholipid contents of the vesicle suspensions were determined by the phospholipid B test from Wako Pure Chemical Industries (Osaka, Japan). Sodium cholate and imidazole were from Serva (Heidelberg) and Sigma, respectively. All other reagents were obtained from Merck or BDH (analytical grade). Dialysis tubing was purchased from Serva and Medicell International (London, U.K.).

2.2. Vesicle preparation

Lipid vesicles were prepared from synthetic dioleoylphosphatidylcholine as described previously using a detergent dialysis method with sodium cholate, producing homogeneous unilamellar vesicles with an average outer diameter of 72 nm [11,12]. All vesicle suspensions were prepared in a buffer containing 30 mM imidazole and various amounts of Na_2SO_4 and K_2SO_4. The pH of the buffer was adjusted to 7.2 with H_2SO_4. Vesicle concentrations were estimated by dividing the lipid concentration by the average number of lipid molecules per vesicle, which was calculated as described previously [9] from the vesicle radius and the partial specific volume of lipid to be 45 200.

2.3. Stopped-flow measurements

Kinetic data for the interaction of oxonols V and VI with dioleoylphosphatidylcholine vesicles and their response to a change in membrane potential have been reported previously and the experimental fluorescence stopped-flow technique is described in detail elsewhere [9]. Briefly, two types of experiments were performed. The interaction of the dyes with vesicles was investigated by mixing a dye solution with an equal volume of vesicle suspension and monitoring the consequent fluorescence change. In order to investigate the response of the dyes to a change in membrane potential, stopped-flow experiments were performed in which a voltage jump was produced. This was achieved by equilibrating a suspension of vesicles with dye and valinomycin in a buffer containing a low K^+ concentration and then mixing this with an equal buffer volume containing a

much higher K^+ concentration. At a sufficiently high valinomycin concentration, a diffusion potential (inside positive) for K^+ could thus be generated within the mixing time [31–33], and the fluorescence response to this voltage jump was then monitored.

Computer simulations of the stopped-flow transients were performed using a Digital VAX computer. The differential forms of the rate equations were integrated using backward differentiation formulae [13] within a subroutine of the Numerical Algorithms Group (NAG) Fortran Library.

2.4. Static fluorescence and absorbance measurements

Fluorescence measurements were carried out in a Perkin-Elmer LS 50 luminescence spectrometer with a thermostatically controlled cuvette holder. The excitation wavelength was set to 580 nm (slit width 15 nm) and the emission was recorded at wavelengths greater than or equal to 600 nm (slit width 20 nm). The oxonol V stock solution contained 0.27 mM dye in ethanol. 2 μl of this solution was added to 2 ml of buffer in the cuvette to obtain a final (total) oxonol concentration of 270 nM. The fluorescence spectrum was then recorded before and after the addition of varying aliquots of vesicle suspension.

Absorbance measurements were carried out in a Varian Cary 219 spectrophotometer with a thermostatically controlled cuvette holder. Spectrophotometric titrations were performed at constant dye concentration and varying vesicle concentration as well as constant vesicle concentration and varying dye concentration.

3. Equilibrium results

On addition of vesicles to a solution of oxonol V, the dye exhibits a red shift of its absorbance maximum of approx. 20 nm and a slight increase in its molar absorptivity at λ_{max} (see fig. 2). An isosbestic point is observed at approx. 613 nm. Titration of vesicles with dye shows that as the dye concentration increases there is a decrease in the magnitude of the absorbance change due to the vesicles, indicating that the vesicles are saturable with dye (see fig. 3). Thus, it seems that the most appropriate description of the dye-vesicle interaction is a binding mechanism, whereby dye binds to vesicles possessing a discrete number of binding sites [14–16]. A partition mechanism involving the transfer of dye from an aqueous to a lipid phase can be excluded, since it predicts a constant ratio between the dye concentrations in the two phases and thus does not allow for the possibility of saturation. Accordingly, the spectral data have been interpreted using the Langmuir adsorption isotherm [17–19]:

$$\bar{r} = \frac{nK\bar{C}_D}{1 + K\bar{C}_D} \tag{1}$$

where $\bar{r}$ is the equilibrium concentration of bound dye per unit concentration of vesicles, n the number of binding sites per vesicle, $\bar{C}_D$ the equilibrium concentration of free dye, and K the association constant for the reaction:

$$\text{Dye} + \text{free binding site} \overset{K}{\rightleftharpoons} \text{occupied site} \tag{2}$$

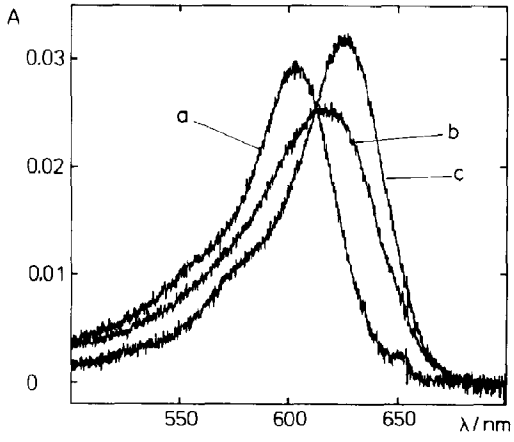

Fig. 2. Variation of the oxonol V absorbance spectrum in the presence of dioleoylphosphatidylcholine vesicles; $T = 22°C$, pH 7.2 (a) 266 nM oxonol V alone, (b) 266 nM oxonol V + 3080 nM lipid, (c) 266 nM oxonol V + 30 800 nM lipid.

Thus, the association constant is defined by

$$K = \frac{[\text{occupied sites}]_{eq}}{\bar{C}_D[\text{free sites}]_{eq}} \quad (3)$$

Combining the absorbance data from dye and vesicle titrations, values of $\bar{r}$ and $\bar{C}_D$ can be calculated and plotted according to the Scatchard relationship (see fig. 4), from which n and K can be determined from the intercept and slope, respectively [20]. The value of $\bar{r}$ has been expressed as the concentration of bound dye per unit concentration of lipid, so that the intercept, y, represents the number of binding sites per lipid molecule rather than the number of sites per vesicle. The values found are:

$K = 3.31(\pm 0.22) \times 10^6\ \text{M}^{-1}$

$y = 0.161(\pm 0.003)$ sites per lipid molecule

The value of y indicates that in a fully saturated vesicle there are $1/y \approx 6$ lipid molecules for every bound dye molecule. These values are comparable to those reported elsewhere [19] for the binding of oxonol V to soybean lipid and dipalmitoyl lecithin vesicles.

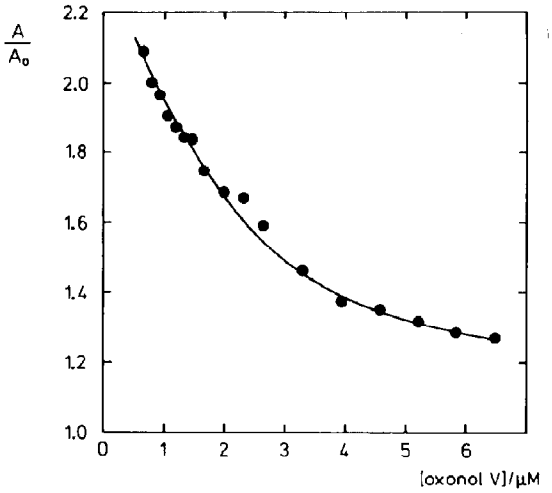

Fig. 3. Absorbance A of oxonol V at 625 nm as a function of dye concentration at a constant total lipid concentration of 7710 nM. A is referred to the absorbance, A_0, at zero lipid concentration.

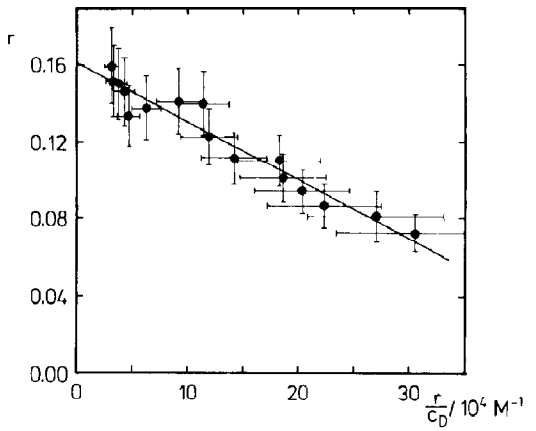

Fig. 4. Scatchard plot for the equilibrium binding of oxonol V to dioleoylphosphatidylcholine vesicles ([lipid] = 7710 nM). The binding of oxonol V was calculated from the absorbance change at 625 nm. r represents the concentration of bound dye per unit concentration of lipid.

Fluorescence titration of oxonol V with vesicles has also been performed (see fig. 5). Again there is a red shift of the dye's spectrum on binding to the lipid and a fluorescence enhancement is apparent. It should be noted, however, that no isosbestic point is observed, suggesting that the fluorescence spectrum of bound dye varies with the extent of binding to the vesicles. For this reason the calculation of K and y has been carried out using absorbance measurements alone.

4. Kinetic theory

Now let us consider the kinetics of the interaction of dye with vesicles utilising the idea of the occupation of binding sites. The kinetic processes of binding and diffusion are shown schematically in fig. 6. The rate constants k_+ and k_- refer to the association and dissociation reactions of dye with a given binding site (see reaction 2), so that $K = k_+/k_-$. The rate constants k' and k'' refer to diffusion across the membrane towards the intravesicular space and towards the external solution, respectively. It is furthermore assumed that in the absence of an electrical potential gradient

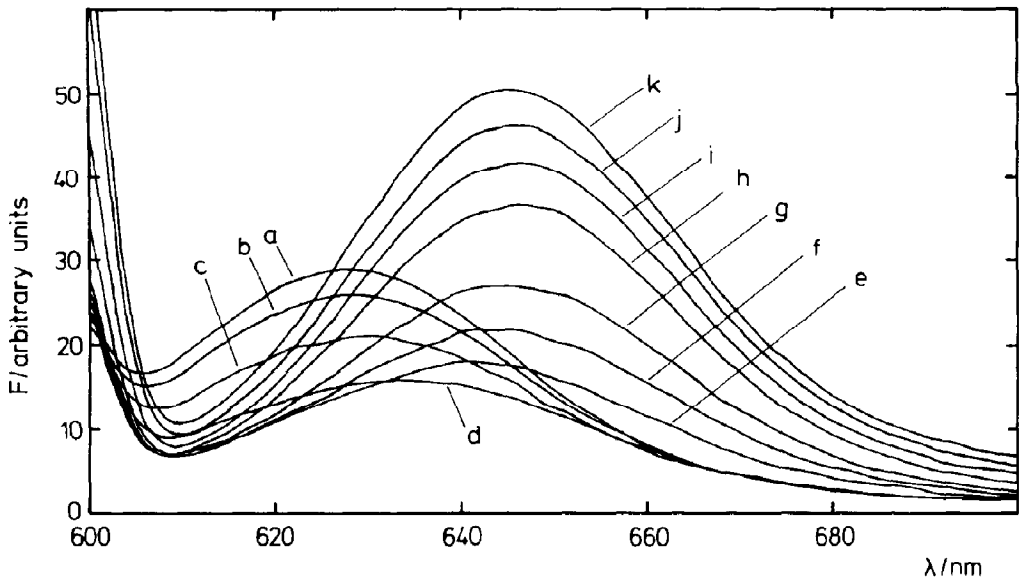

Fig. 5. Variation of the oxonol V fluorescence spectrum in the presence of dioleoylphosphatidylcholine vesicles; $T = 22\,^{\circ}C$, pH 7.2. (a) 266 nM dye alone, (b–k) after the addition of vesicles to final lipid concentration in the range 125–30900 nM.

across the membrane the values of k' and k'' are equal.

4.1. Binding alone

First let us consider binding of dye to the exterior of the vesicles, neglecting diffusion to begin with. For the binding of dye, D, to a vesicle,

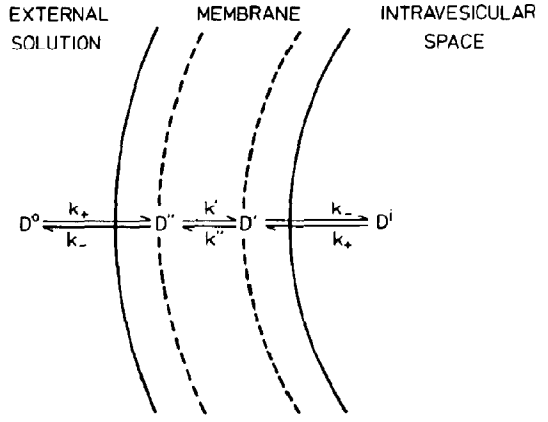

Fig. 6. Binding and diffusion steps for the interaction of an oxonol dye with the vesicle membrane.

V, with n binding sites one can write the following reaction scheme:

$$\begin{aligned} &\mathrm{D} + \mathrm{V} \underset{k_-}{\overset{nk_+}{\rightleftharpoons}} \mathrm{DV} \\ &\mathrm{D} + \mathrm{DV} \underset{2k_-}{\overset{(n-1)k_+}{\rightleftharpoons}} \mathrm{D_2V} \\ &\mathrm{D} + \mathrm{D_2V} \underset{3k_-}{\overset{(n-2)k_+}{\rightleftharpoons}} \mathrm{D_3V} \\ &\quad\vdots \end{aligned} \tag{4}$$

Implicit in these relations is the assumption that there are no interactions between the dye molecules in the lipid membrane, so that the dye association rate constant for each step changes merely by a statistical factor corresponding to the initial number of empty sites on the vesicle. The backward rate constant changes by a statistical factor corresponding to the number of occupied sites after binding. The total concentration of dye bound to the lipid, C^*_{DV}, and that of the vesicles, C^*_V, are given by

$$C^*_{DV} = C_{DV} + 2C_{D_2V} + 3C_{D_3V} + \ldots \tag{5}$$

$$C^*_V = C_V + C_{DV} + C_{D_2V} + C_{D_3V} + \ldots \tag{6}$$

Based upon the reaction scheme above and utilising eqs 5 and 6 it can be shown that the overall rate of change of concentration of bound dye is given by

$$\frac{dC^*_{DV}}{dt} = nk_+C_DC^*_V - (k_+C_D + k_-)C^*_{DV} \quad (7)$$

Now let us introduce the term

$$r = \frac{C^*_{DV}}{C^*_V} \quad (8)$$

which represents the ratio of bound dye to the total vesicle concentration at any time during the reaction and in terms of binding sites corresponds to the number of free sites per vesicle. Substituting for C^*_{DV} from eq. 8 in eq. 7 yields,

$$\frac{dr}{dt} = nk_+C_D - (k_+C_D + k_-)r \quad (9)$$

We now introduce the total dye concentration C^*_D:

$$C^*_D = C_D + C^*_{DV} \quad (10)$$

Combining eqs 9 and 10 with the definition of K given above in eq. 3 eventually yields

$$\frac{dr}{dt} = -\left[(n-r)k_+C^*_V + \frac{n}{n-\bar{r}}k_-\right](r-\bar{r}) \quad (11)$$

$$\bar{r} = \frac{K(n-\bar{r})C^*_D}{K(n-\bar{r})C^*_V + 1} \quad (12)$$

where $\bar{r}$ designates the equilibrium value of r. Under conditions of great excess of vesicles, i.e., $n \gg r$, eqs 11 and 12 reduce to the forms previously derived [9] for the case where saturation of binding sites can be neglected. As previously reported elsewhere [21], integration of eq. 11 yields the following expression for r as a function of time:

$$r = \frac{b\bar{r}(1-e^{at})}{\bar{r}k_+C^*_V - be^{at}} \quad (13)$$

where

$$a = (n-\bar{r})k_+C^*_V + \frac{n}{n-\bar{r}}k_- \quad (14)$$

$$b = \frac{n\left[(n-\bar{r})k_+C^*_V + k_-\right]}{n-\bar{r}} \quad (15)$$

Eqs 13–15 are quite general expressions which explain the time course of the binding of any dye to the exterior of lipid vesicles. They are, however, only applicable to cases where diffusion across the membrane can be neglected, e.g., if diffusion occurs on a much longer time scale than binding, so that the binding step can be considered to be completely decoupled from diffusion or the dye is membrane impermeable. When diffusion and binding are considered together, one obtains, as will be shown shortly, a series of coupled differential equations for the various dye environments, and direct integration of the rate equations is no longer possible.

Before discussing diffusion let us first consider the fluorescence change observed due to dye binding. The fluorescence, F, and any time, t, can be defined by the following equation:

$$F = C_Df_w + C^*_{DV}f_l \quad (16)$$

where f_w and f_l are the values of fluorescence intensity per mole of dye in water and bound to the lipid, respectively. If f_w and f_l are both considered to be constants, it can be shown [9] that the fluorescence signal, when dye and vesicles are mixed in a stopped-flow experiment, should follow a time course governed by a relaxation time, τ, given by

$$1/\tau = (n-r)k_+C^*_V + \frac{n}{n-\bar{r}}k_- \quad (17)$$

If experiments are performed at great excess of vesicle binding sites over dye molecules such that $n \gg r$, eq. 17 reduces to

$$1/\tau = nk_+C^*_V + k_- \quad (18)$$

which is of the same form as the equation derived in a previous paper [9] for conditions of excess vesicle concentrations. In this case a single exponential relaxation would be expected, and a plot of the reciprocal relaxation time vs the total vesicle concentration should yield a straight line, from which the rate constants nk_+ and k_- can be determined from the slope and intercept, respectively. The expression nk_+ represents the rate constant for binding of a dye molecule to a vesicle with n binding sites.

Eqs 11–15 described above are in fact quite

general, irrespective of the means of detecting the binding reaction, and eq. 17 could equally well be applied to absorbance measurements. In the case of fluorescence detection, however, the actual course of the fluorescence change during the binding process may become more complicated at high dye/lipid concentration ratios, because the fluorescence of a dye molecule in the lipid may be affected by the proximity of neighbouring dye molecules. This would seem to be apparent in the stopped-flow experiments of the binding of oxonol V [9,21] and oxonol VI (H.J. Apell, unpublished results) with lipid vesicles as a reversal of the sign of the fluorescence change after an initial rise, if the experiments are performed at a sufficiently high dye concentration. Thus, in eq. 16, f_l may not in fact be a constant, but instead it may vary with the value of r, e.g., a dye molecule binding to a lipid binding site may be expected to have a higher fluorescence if it binds in a region free of other dye molecules than if it binds next to an already bound dye molecule, because of the likelihood of self-reabsorption of the light quanta. As an approximation let us assume that there are only two possible fluorescence states of dye within the lipid:

(1) dye isolated, with fluorescence intensity f_l^i

(2) dye bound next to another dye molecule, with fluorescence intensity f_l^q (i.e., quenched)

Let us now introduce the quantity P_i, the probability that a given dye molecule in the lipid is isolated, which is a function of r. The fluorescence of dye in the lipid, f_l, at any given value of r is then given by

$$f_l = f_l^i P_i + f_l^q (1 - P_i) \tag{19}$$

Now substituting this expression for f_l into eq. 16 and replacing C_D by $C_D = C_D^* - C_{DV}^*$ as well as C_{DV}^* by $C_{DV}^* = rC_V^*$, one obtains the result that the fluorescence change during the course of the reaction is described by

$$F - F_0 = C_V^* r \left[f_l^q + P_i \left(f_l^i - f_l^q \right) - f_w \right] \tag{20}$$

where F_0 ($\equiv C_D^* f_w$) is the initial fluorescence of the dye solution before any binding to the vesicles has occurred. Now in order to evaluate this expression for varying values of r, the dependence of P_i on r is required.

Consider the binding sites to be arranged on a two-dimensional lattice over the vesicle, where each binding site is surrounded by z nearest neighbours. The probability that a certain binding site is occupied is given by r/n. Therefore, the probability that a given binding site is free is expressed by $(1 - r/n)$. The probability that for a given bound dye molecule all the neighbouring binding sites are unoccupied is then given by

$$P_i = \left(1 - \frac{r}{n}\right)^z \tag{21}$$

For any given experimental conditions, combination of eqs 12–15, 20, and 21 allows the computer simulation of stopped-flow experiments [21]. Good agreement between the experimental and simulated time course of the fluorescence change due to the binding of oxonol V to lipid vesicles has been achieved [21].

4.2. Binding followed by diffusion

Now let us consider the more complete situation for the oxonol dyes, where binding is followed by diffusion of the dye to binding sites in the inner monolayer of the vesicle (see fig. 6). There are now two classes of binding sites, those in the outer and those in the inner monolayer, and two aqueous concentrations of dye to be considered, the extra- and intravesicular concentrations. Thus, let us make the following definitions:

n_0 ≡ number of binding sites in the external monolayer per vesicle

n_i ≡ number of binding sites in the internal monolayer per vesicle

$N_D^0 = C_D^0 / C_V^* \equiv$ number of molecules of dye in the extravesicular solution per vesicle

$N_D^i = C_D^i V_i L \equiv$ number of molecules of dye in the intravesicular solution per vesicle

r_0 ≡ number of external binding sites occupied per vesicle

r_i ≡ number of internal binding sites occupied per vesicle.

The quantities C_D^0 and C_D^i refer to the molar concentrations of dye in the external and internal solution, respectively, V_i being the volume of the

intravesicular space of a single vesicle, and L denotes Avogadro's constant.

The concentration of dye in the internal and external monolayers can be expressed in terms of the fraction of binding sites occupied, i.e., r_0/n_0 for the externally bound dye and r_i/n_i for the internally bound dye. Considering for the moment diffusion alone, the change in concentration of dye in the internal monolayer with time is then given by

$$\frac{d(r_i/n_i)}{dt} = k' \frac{r_0}{n_0} - k'' \frac{r_i}{n_i} \tag{22}$$

Rearrangement then yields,

$$\frac{dr_i}{dt} = k' \frac{n_i}{n_0} r_0 - k'' r_i \tag{23}$$

Similarly, it can be shown that for externally bound dye the rate of change of r_0 due to diffusion alone is given by

$$\frac{dr_0}{dt} = k'' \frac{n_0}{n_i} r_i - k' r_0 \tag{24}$$

In order to obtain expressions for the rate of change of concentrations of all dye species due to the combined effects of binding, dissociation, and diffusion, eqs 23 and 24 can now be combined with eq. 9 for binding and dissociation alone. Thus, one obtains the following series of coupled differential equations.

$$\frac{dN_D^0}{dt} = -n_0 k_+ N_D^0 C_V^* + \left(k_+ N_D^0 C_V^* + k_-\right) r_0 \tag{25}$$

$$\frac{dr_0}{dt} = n_0 k_+ N_D^0 C_V^* - \left(k_+ N_D^0 C_V^* + k_-\right) r_0 + k'' \frac{n_0}{n_i} r_i - k' r_0 \tag{26}$$

$$\frac{dr_i}{dt} = n_i k_+ \frac{N_D^i}{LV_i} - \left(k_+ \frac{N_D^i}{LV_i} + k_-\right) r_i + k' \frac{n_i}{n_0} r_0 - k'' r_i \tag{27}$$

$$\frac{dN_D^i}{dt} = -n_i k_+ \frac{N_D^i}{LV_i} + \left(k_+ \frac{N_D^i}{LV_i} + k_-\right) r_i \tag{28}$$

Calculation of the concentrations of the various species at any point in time can be simplified, i.e., one differential equation can be omitted, by utilising the mass action law,

$$\frac{C_D^*}{C_V^*} = N_D^0 + r_0 + r_i + N_D^i \tag{29}$$

If eqs 25–29 are solved for given values of the rate constants, numbers of internal and external binding sites and vesicle and dye concentrations, the time course of the fluorescence can be calculated using equations analogous to those derived (eqs 20 and 21) in section 4.1. Thus, assuming that the fluorescence of an isolated dye molecule in the external and internal monolayers is identical, the fluorescence at any point in time is given by

$$F = C_D^* f_w + C_V^* r_0 \left[f_1^d + P_i^0 \left(f_1^i - f_1^d\right) - f_w\right] + C_V^* r_i \left[f_1^d + P_i^i \left(f_1^i - f_1^d\right) - f_w\right] \tag{30}$$

where P_i^0 and P_i^i are the probabilities that an externally and an internally bound dye molecule, respectively, are isolated and are given by

$$P_i^0 = \left(1 - \frac{r_0}{n_0}\right)^z \tag{31}$$

$$P_i^i = \left(1 - \frac{r_i}{n_i}\right)^z \tag{32}$$

Up to now, however, the fact that the dyes are charged has been neglected. For a complete description of the experimental behaviour and for the simulation of stopped-flow kinetic traces either with or without a voltage jump, the effect of the charge must be taken into account.

4.3. Electrical effects

An important point affecting the rate of diffusion of hydrophobic ions across the membrane is the presence of electrical potential gradients. Thus, because the dyes are charged, the rate of diffusion can be accelerated or decelerated depending on the sign and magnitude of an electrical potential difference across the membrane. In the case of vesicles this could come about if the membrane is selectively permeable to a particular ion, so that a diffusion potential is created if a concentration difference exists on the two sides of the membrane. The diffusion of dye between the two classes

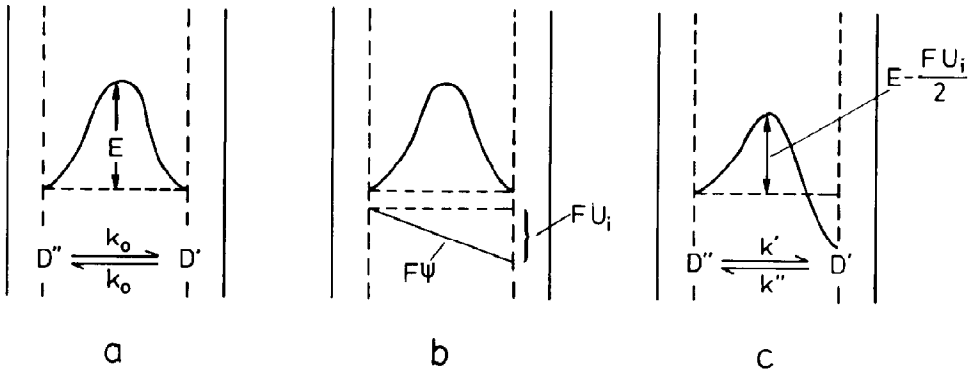

Fig. 7. Energy profile of an oxonol dye molecule in a lipid membrane. (a) Symmetric energy barrier in the absence of an electrical potential gradient; (b, c) production of an asymmetric barrier in the presence of an electrical potential gradient. (Adapted from Fig. 10.30 of ref. 29.)

of sites, because of its charge, also causes a current within the membrane, so that a separate electrical potential gradient inside the membrane exists which also modifies the rate of diffusion.

The movement of dye molecules across the membrane may be described as a translocation over a symmetrical Eyring barrier [22]. Upon binding of dye to sites on the membrane, however, because of the charge on the dye, an electrical potential difference across the membrane interior will be produced and the energy barrier will become skewed to one side (see fig. 7). Accordingly, the diffusion rate constants k' and k'' are given by

$$k' = k_0 \exp\left(\frac{FU_i}{2RT}\right) \tag{33}$$

$$k'' = k_0 \exp\left(-\frac{FU_i}{2RT}\right) \tag{34}$$

where $U_i = \psi_i' - \psi_i''$ is the potential difference between the interior and exterior binding sites and k_0 the rate constant at zero voltage. Since U_i changes as dye binds and moves across the membrane, the values of k' and k'' will continually be changing until equilibrium is reached. Thus, an expression for dU_i/dt is required.

Let us apply the three-capacitor model (see fig. 8), which has previously been used for the adsorption of lipophilic ions to lipid bilayers [23–25]. The dye is assumed to bind to adsorption planes located symmetrically with respect to the centre of the membrane. Thus, the membrane can be considered to be analogous to a system of three capacitors in series, where C_0 is the electrical capacitance of the two regions between the adsorption planes and the adjacent aqueous solu-

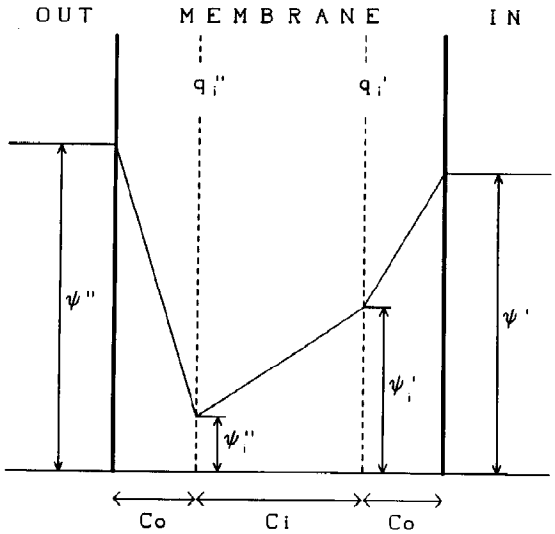

Fig. 8. Three-capacitor model. The dye is assumed to bind to adsorption planes located symmetrically with respect to the centre of the membrane. C_0 is the electrical capacitance between the adsorption plane and the adjacent aqueous solution. C_i is the electrical capacitance between the two adsorption planes. ψ'', ψ_i'', ψ_i' and ψ' are the electrical potentials, and q_i'' and q_i' are the charge densities of dye in the adsorption planes.

tions, and C_i that between the two adsorption planes in the membrane interior. The capacitance C_0 is also taken to include a small contribution from the capacitance of the electrical double layer of the adjacent aqueous solution [24]. According to fig. 8 one can define the following potential differences across the various regions of the membrane,

$$U' = \psi' - \psi_i' \tag{35}$$

$$U'' = \psi_i'' - \psi'' \tag{36}$$

$$U_i = \psi_i' - \psi_i'' \tag{37}$$

$$U_m = \psi' - \psi'' \tag{38}$$

where U' and U'' are the internal and external boundary potentials, U_i the potential difference across the membrane interior, and U_m the total membrane potential. It can easily be shown that the total membrane potential is simply given by the sum of the potential differences of the individual regions, i.e.,

$$U_m = U' + U'' + U_i \tag{39}$$

For the three capacitors in series the total membrane capacitance, C_m, is related to C_0 and C_i by

$$\frac{1}{C_m} = \frac{2}{C_0} + \frac{1}{C_i} \tag{40}$$

On the basis of the model [23–25] the charge densities, q_i' and q_i'', in the adsorption planes are given according to Gauss' law [30] by

$$q_i' = C_i U_i - C_0 U' \tag{41}$$

$$q_i'' = C_0 U'' - C_i U_i \tag{42}$$

Combination of eqs 39–42 then leads to

$$U_i = U_m - \frac{1}{C_0}(q_i'' - q_i') \tag{43}$$

The charge densities can be estimated from the number of binding sites occupied and the internal and external surface areas of the vesicle, i.e.,

$$q_i'' = -\frac{e_o r_o}{A_o};\ q_i' = -\frac{e_o r_i}{A_i} \tag{44}$$

Let us also define a quantity $\alpha \equiv C_m/C_0$, whose value is such that $0 < \alpha \leqq 0.5$. Substituting α and the expressions for q into eq. 43 then yields

$$U_i = U_m + \frac{\alpha e_o}{C_m}\left(\frac{r_o}{A_o} - \frac{r_i}{A_i}\right) \tag{45}$$

The quantity α is a parameter which must be experimentally determined. If the membrane were a completely homogeneous dielectric medium, the value of α would be equal to the ratio of the distance of an adsorption plane from its adjacent aqueous interface to the thickness of the membrane. Thus, a value of 0 would correspond to the situation where the adsorption planes are located directly at the membrane-solution interfaces and 0.5 to the situation where there is a single adsorption plane located in the centre of the membrane. More realistically, however, the dielectric constant probably varies across the width of the membrane, and hence it is not possible to determine from the value of α alone exactly where the adsorption planes lie in relation to the membrane-solution interface.

Differentiating eq. 45 with respect to time yields,

$$\frac{dU_i}{dt} = \frac{\alpha e_0}{C_m}\left(\frac{1}{A_0}\frac{dr_0}{dt} - \frac{1}{A_i}\frac{dr_i}{dt}\right) \tag{46}$$

Here it has been assumed that the amount of dye which dissociates into the intravesicular space is so small that no significant change in U_m occurs. Eq. 46 can now be added to the series of coupled differential equations previously derived (eqs 25–28).

5. Simulated and experimental results

Using the equations derived in section 4 the time course of the fluorescence change of the dye as it binds to the vesicles and diffuses across the membrane can be simulated on the computer and comparison to experimentally obtained fluorescence transients can be made. In the case of the experiments described in section 2.3., in which dye and vesicles were simply mixed in the stopped-flow

apparatus, the simulation has been carried out using the following procedure:

(1) For given values of C_D^*, C_V^*, n_o, n_i, k_+, k_-, k_0, A_0, A_i, C_m, and V_i integrate eqs 26–28 and 46 to obtain N_D^0, r_0, r_i, N_D^i and U_i as a function of time. This also requires the use of eq. 29 for the calculation of N_D^o and eqs 33 and 34 for the variation of the diffusion rate constants with U_i. A value of α must be assumed.

(2) From the values of r_0 and r_i calculate P_i^0 and P_i^i from eqs 31 and 32 using an assumed value of z.

(3) Calculate F as a function of time from eq. 30 using the previously calculated values of r_0, r_i, P_i^0 and P_i^i.

The initial values of r_0, r_i, N_D^i and U_i before any dye has bound are set to zero. The values of n_0 and n_i were determined from the total number of binding sites per vesicle and were divided into the two classes based upon the ratio of the external and internal vesicle surface areas. All calculations were for a standard monodisperse vesicle population with an external vesicle radius of 36 nm and a membrane thickness of 4 nm. The value of z was chosen after trying several small integral values, with 3 seeming to give the best correlation between the experimental and simulated data [21].

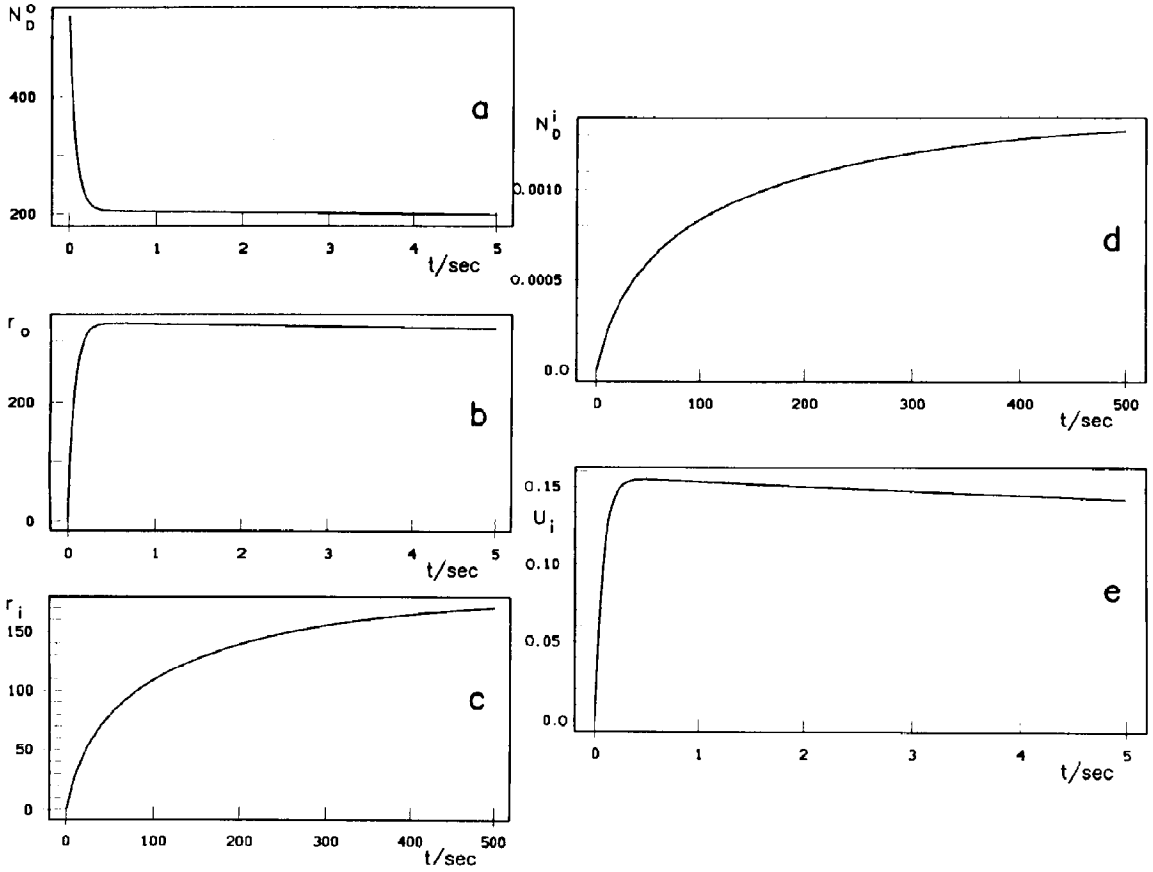

Fig. 9. Computer simulations of the variation with time of (a) N_D^o (dye molecules per vesicle), (b) r_o (binding sites occupied per vesicle), (c) r_i (binding sites occupied per vesicle), (d) N_D^i (dye molecules per vesicle) and (e) U_i (V), at a total oxonol V concentration of 75 nM and a total vesicle concentration of 0.14 nM.

For oxonol V the most appropriate value of α was found to be approx. 0.48. Based on calculations of the potential dependence of the equilibrium binding of oxonol VI to vesicles, a value of 0.2 for α has been reported [25]. Thus, it would seem that oxonol V binds at a position further towards the centre of the membrane than oxonol VI. The variation of N_D^0, r_0, r_i, N_D^i and U_i with time, calculated using the above procedure for particular dye and vesicle concentrations, is shown in fig. 9. As would be expected N_D^0 decreases and r_0 increases rapidly as soon as binding starts. For N_D^0 this is followed by a slower decrease as dye moves across the membrane and there is a readjustment of the binding equilibrium, resulting in a further decrease in the amount of free dye. Similarly, for r_0 the rapid increase is followed by a slower decrease as the dye distributes itself between the binding sites on both sides of the membrane. For r_0 and N_D^i there is an initial lag which occurs in the first 0.2 s, but because of the time scale this is not apparent in fig. 9. The lag is due to the fact that diffusion across the membrane must first occur before any change is observed. After this lag phase r_i and N_D^i both increase until eventually equilibrium is reached. For r_i the increase is simply due to diffusion across the membrane, whereas for N_D^i this is followed by dissociation into the intravesicular space. Because of the high affinity of oxonol V for the lipid phase, it can be seen that at these concentrations N_D^i reaches a level of on average only approx. 0.0014 dye molecules per vesicle. The effect that this dye current across the membrane would have on the membrane potential can be estimated from the membrane capacitance. Thus,

$$U_m = \frac{-\Delta N_D^i e_0}{C_m A}$$

$$= \frac{-0.0014 \times 1.6 \times 10^{-19}}{1 \times 10^{-6} \times 4\pi \times 36 \times 10^{-7} \times 32 \times 10^{-7}}$$

$$= -1.5 \times 10^{-6}\ \text{V} = -0.0015\ \text{mV}$$

Accordingly this tiny effect of the dye on the membrane potential has been neglected and U_m is assumed to be constant. As can be seen from fig. 9, however, the dye has a dramatic effect on the potential across the membrane interior. Initially there is a rapid rise in U_i as negatively charged dye binds to the external binding sites and then there is a slower decay in U_i as dye moves across the membrane and the negative charge is distributed between the sites on both sides of the membrane. In fig. 10, experimental and simulated fluorescent transients are shown for comparison. Both show an initial rapid increase in fluorescence due to the binding step followed by a slower increase as dye diffuses across the membrane. In the calculations it has been assumed that the fluorescence of an isolated dye molecule in the external and internal monolayers is identical. The fact that diffusion still results in a change in fluorescence is due to two factors. Firstly, because the diffusion reaction

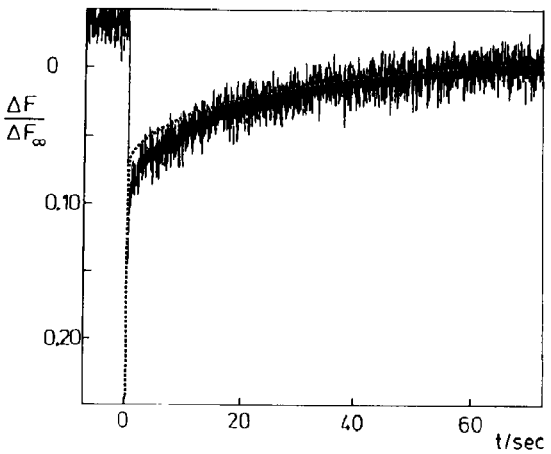

Fig. 10. Stopped-flow traces. (Solid line) Experimental stopped-flow trace. Oxonol V in buffer containing 75 mM K_2SO_4 and vesicles in buffer containing 75 mM K_2SO_4 were mixed to final concentrations of 75 nM dye and 0.14 nM vesicle (lipid concentration 6.3 μM); $T = 22\,^\circ$C, pH 7.2. (Dashed line) Computer simulation of a fluorescence stopped-flow trace using eqs 26–34 and 46. Values of the parameters used are: $C_D^* = 7.5 \times 10^{-8}$ M, $C_V^* = 1.4 \times 10^{-10}$ M, $k_+ = 1.6 \times 10^7$ M^{-1} s^{-1}, $k_- = 4.7$ s^{-1}, $n_o = 3.86 \times 10^3$ external sites per vesicle, $n_i = 3.44 \times 10^3$ internal sites per vesicle, $k_o = 0.0006$ s^{-1}, $C_m = 1 \times 10^{-6}$ F cm^{-2}, $f_w = 7.15 \times 10^7$ (arbitrary units) M^{-1}, $f_l^i = 19.08 \times 10^7$ (arbitrary units) M^{-1}, $f_l^a = 0$ (arbitrary units) M^{-1}, $A_o = 1.63 \times 10^{-10}$ cm^2, $A_i = 1.29 \times 10^{-10}$ cm^2, $V_i = 8.27$ dm^3 mol^{-1}, $\alpha = 0.48$ and $z = 3$. The simulated curve has been normalized to the fluorescence change of the experimental trace. On the time scale of the figure the simulated and experimental curves show an identical initial rapid increase in fluorescence over the first fraction of a second.

is coupled to the binding step, the movement of dye across the membrane results in a readjustment of the equilibrium between free and externally bound dye, causing an overall increase in the amount of bound dye and hence a fluorescence change. Secondly, at high dye concentrations the diffusion reaction by itself would cause an increase in fluorescence, because it results in the equal distribution of dye between the external and internal binding sites and hence a minimisation of the degree of quenching.

The dependence of the apparent reciprocal relaxation time for the diffusion reaction on vesicle and dye concentration has been measured previously (see fig. 4 in ref. 9). It was suggested [9] that the dramatic acceleration of the diffusion rate at high dye/lipid concentration ratios might be due to a perturbation of the membrane structure as dye accumulates in the membrane, however, this can now be attributed to quenching, which causes a fluorescence plateau to be reached earlier than would otherwise be the case, resulting in an overestimate of the reciprocal relaxation time. This can be seen from the simulated kinetic plots (see fig. 11), where calculations of the apparent reciprocal relaxation times have been carried out including and excluding quenching. For each simulated fluorescence curve the reciprocal relaxation time has been estimated from the slope of a semilogarithmic plot vs time of the difference in fluorescence at any time from its maximum value. Simulations in which quenching was ignored were performed by setting $f_1^q = f_1^i$ in the calculation. Similar apparent accelerations of the binding reaction at high dye/lipid concentration ratios have also been found which are likewise attributable to quenching [21]. In the case of the diffusion reaction, however, at low dye/lipid concentration ratios there is still a smaller increase of the reciprocal relaxation time with the dye/lipid ratio, which cannot be attributed to quenching since it is observed even in simulations in which quenching is ignored (see fig. 11). This can be explained by the electrical potential gradient generated across the interior of the membrane by the binding of the dye. As the dye concentration increases, the difference in the degree of occupation of the external and internal binding sites shortly after mixing also

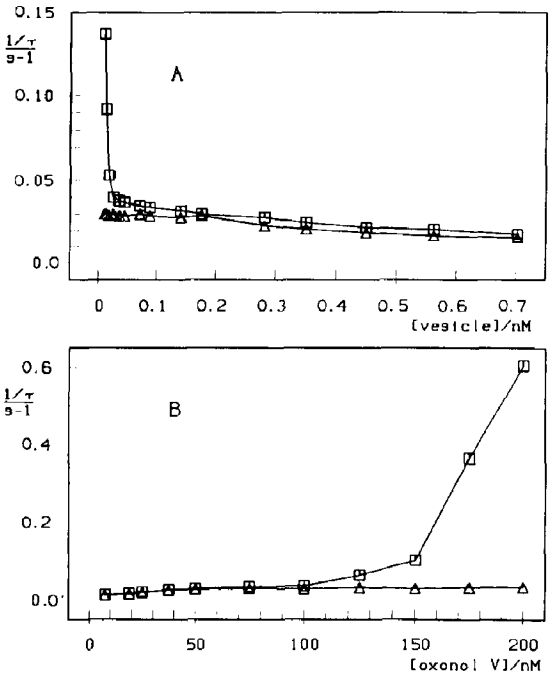

Fig. 11. Simulated kinetic plots for the diffusion reaction of oxonol V with vesicles. (A) Dependence of the reciprocal relaxation time on vesicle concentration. [Oxonol V] = 75 nM. (B) Dependence of the reciprocal relaxation time on oxonol V concentration. [Vesicle] = 0.070 nM. The rectangular data points are derived from simulations where quenching is included, the triangular data points refer to simulations where quenching is neglected ($f_1^q = f_1^i$). The values of parameters, except for the concentrations, are as given in fig. 10.

increases, producing a greater positive potential difference across the membrane interior and thus an acceleration of the initial rate of diffusion.

For the second type of stopped-flow experiment in which the fluorescence response of the dye to a rapid change in membrane potential was investigated (see section 2.3), simulations were also carried out. In this case, the equilibrium values of N_D^o, r_o, N_D^i and U_i were first determined with $U_m = 0$ using the procedure 1–4 above until no further change in their magnitudes was apparent. These values were then input as initial values, the voltage jump required was added to the value of U_i according to eq. 45, and the procedure 1–4 was once more carried out to give the simulated voltage response. Experimental and simulated fluo-

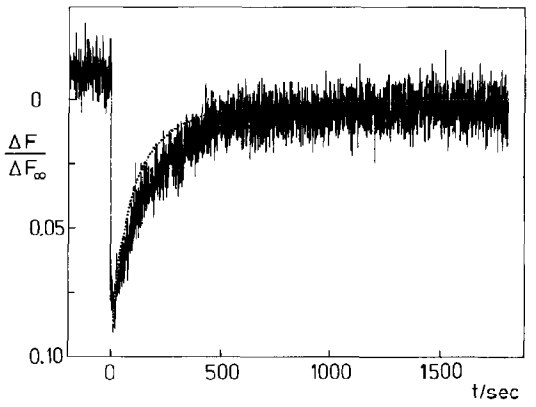

Fig. 12. Voltage-jump stopped-flow traces. (Solid line) Stopped-flow experiment in which a suspension of vesicles equilibrated with oxonol V and valinomycin and in a buffer containing 2.5 mM K_2SO_4 and 72.5 mM Na_2SO_4 was mixed with a buffer containing 75 mM K_2SO_4. The membrane potential produced was 66 mV. Final concentrations were: [oxonol V] = 75 nM, [vesicle] = 0.14 nM, [valinomycin] = 16.5 nM. T = 22° C, pH 7.2. (Dashed line) Computer simulation of a voltage-jump fluorescence stopped-flow trace using eqs 26–34, 45 and 46 as described in the text. Values of the parameters used are as given in fig. 10 except that U_m = 66 mV. The simulated curve has been normalized to the fluorescence change of the experimental trace.

rescent transients for voltage jump experiments are shown in fig. 12. In this case only a single kinetic process is observed, which is the redistribution of dye over the membrane according to the new membrane potential. The binding of dye which occurs subsequent to diffusion is much faster than the diffusion process and hence the binding equilibrium is able to readjust almost instantaneously on the time scale of diffusion.

In order to obtain the best agreement between the experimental and simulated data, the most appropriate value for the diffusion rate constant, k_0, of oxonol V in the absence of a potential difference across the membrane was determined to be:

$$k_0 \approx 6 \times 10^{-4}\ s^{-1}$$

The fact that this is significantly lower than previously reported diffusion rate constants for oxonol V [9] is because these values refer to situations where a potential gradient across the membrane interior, caused by the dye itself, is present, which accelerates the rate of diffusion.

6. Discussion

The interaction of oxonol V and VI with lipid vesicles has been found to proceed via a two-step process involving the rapid binding of dye to the external lipid monolayer, followed by the slower diffusion of dye across the membrane to the internal monolayer [9,21]. Here a kinetic model has been presented which successfully predicts the time course of the fluorescence change due to the dye-vesicle interaction as well as the response to a change in membrane potential.

The first basic feature of the model is that it assumes the presence of saturable binding sites on both sides of the vesicle membrane. This has enabled the dependence of the fluorescence change on the dye/lipid concentration ratio and the sign reversal of the fluorescence change at high dye/lipid ratios to be explained by a decrease in the fraction of isolated dye in the membrane and hence an increase in quenching as the occupation of binding sites increases. It has been suggested that the fluorescence quenching comes about via an inner filter effect due to the increase in local dye concentration in the lipid, however, a direct energy transfer between adjacent dye molecules and loss of energy via intersystem crossing and radiationless transitions is also possible. A similar mechanism of dye-membrane interaction involving the occupation of binding sites has also been proposed by other authors for certain cationic dyes [26,27]. In these cases, however, the quenching has been attributed to the formation of membrane-bound dimers and a dimerisation constant in the membrane has been introduced. The model presented here does not require the assumption of a dimerisation constant, the degree of quenching being calculated from the ratio of the occupied and total numbers of binding sites and their coordination number, z (see eq. 21). It should be noted that for oxonol V and VI there is a significant degree of overlap between the absorbance and fluorescence spectra, and in ethanolic solution the fluorescence of oxonol V alone is only linear

up to a concentration of approx. 2 μM [28]. Because of the large association constant of the dye for the lipid, large local concentrations of dye in the lipid would be expected even with total dye concentrations in the nanomolar range, so that quenching due to an inner filter effect is most likely.

The nature of the binding sites should briefly be discussed. In fact it is inconceivable that a synthetic lipid membrane should have pre-formed binding sites for oxonol dyes. The binding probably proceeds with the dye pushing its way into the lipid bilayer with hydrophobic interactions as the driving force. Nevertheless, it seems that the vesicles are not able to accept an indefinite number of dye molecules. The binding of a dye molecule to the lipid probably causes an expansion of the surface of the bilayer, and due to this process a limit may be reached where the binding of further dye molecules becomes thermodynamically unfavourable, so that the assumption of saturable binding sites provides the best mathematical description of the dye-vesicle interaction.

A second important feature of the kinetic model is that the rate constant for diffusion of dye between the outer and inner binding sites is dependent on the electrical potential gradient across the membrane interior, which is determined by the boundary potentials on both sides of the membrane and the membrane potential (see fig. 8). The degrees of occupation of the internal and external binding sites determine the magnitude of the boundary potentials and hence, in part, the rate constant for movement of dye across the membrane. The rate constant is then potential-dependent and, because the dye is charged, indirectly concentration-dependent. This explains the observation previously reported [9] and mentioned in section 1, that oxonol V moved more slowly through the vesicle membrane in the voltage-jump experiments in comparison to the case when dye and vesicles were mixed in the absence of a membrane potential. For the experiments where dye and vesicles are mixed, as soon as a few dye molecules bind to the external binding sites a large potential difference builds up across the membrane interior which accelerates the movement of dye across to the internal binding sites. In the case of the voltage-jump experiments, however, there is initially already a significant degree of occupation of the internal binding sites, so that a much smaller potential difference across the membrane interior is produced by the movement of dye and hence a smaller rate constant is apparent. For oxonol VI no significant difference in the rate constant for the two types of experiments was observed [9]. This can be explained by a number of contributing factors. Firstly, the lower association constant of oxonol VI in comparison to oxonol V results in a smaller concentration of membrane-bound dye, which would produce much lower boundary potentials and hence a much smaller effect of the dye on the diffusion rate constant. Another factor is that oxonol VI appears to be intrinsically more membrane permeable than oxonol V. Thus, as soon as a dye molecule binds it moves more rapidly through the membrane and less time is available for a potential difference across the interior of the membrane to develop. A third contributing factor is the value of α, which is partially a reflection of how deep inside the membrane the dye binds. Since, as seems to be the case, oxonol VI may not bind as far into the membrane as oxonol V, the potential difference between the two adsorption planes for given concentrations of externally and internally bound dye will be reduced (see eq. 45) and thus the effect on the diffusion rate will also be less.

Finally, it should be noted that the kinetic equations developed here to explain the fluorescence stopped-flow kinetics of oxonol dye-vesicle interaction are of quite general application for the saturable binding and diffusion kinetics of small hydrophobic ions with lipid vesicles.

Acknowledgements

The author would like to thank Professor P. Läuger and Dr H.-J. Apell for many valuable discussions, correspondence, and suggestions concerning this work and for help in preparing the manuscript, and also Frau M. Roudna for the preparation of the diagrams. Financial support from the Alexander von Humboldt-Stiftung and

from the Leverhulme Trust is gratefully acknowledged.

References

1 C.L. Bashford and J.C. Smith, Methods Enzymol. 55 (1978) 569.
2 L.B. Cohen and B.M. Salzberg, Rev. Physiol. Biochem. Pharmacol. 83 (1978) 33.
3 A.S. Waggoner, Annu. Rev. Biophys. Bioeng. 8 (1979) 47.
4 J.C. Freedman and P.C. Laris, Int. Rev. Cytol. Suppl. 12 (1981) 177.
5 A.S. Waggoner, in: The enzymes of biological membranes, 2nd end, ed. A.N. Martonosi (Plenum, New York, 1985) vol. 3, p. 313.
6 T.J. Lampidis, Y. Hasin, M.J. Weiss and L.B. Chen, Biomed. Pharmacother. 39 (1985) 220.
7 D.J. Castro, R.E. Saxton, H.R. Fetterman and P.H. Ward, Otolaryngol. Head Neck Surg. 98 (1988) 581.
8 A.R. Oseroff, D. Ohuoha, G. Ara, D. McAuliffe, J. Foley and L. Cincotta, Proc. Natl. Acad. Sci. U.S.A. 83 (1986) 9729.
9 R.J. Clarke and H.-J. Apell, Biophys. Chem. 34 (1989) 225.
10 J.C. Smith, P. Russ, B.S. Cooperman and B. Chance, Biochemistry 15 (1976) 5094.
11 H.-J. Apell, M.M. Marcus, B.M. Anner, H. Oetliker and P. Läuger, J. Membrane Biol. 85 (1985) 49.
12 M.M. Marcus, H.-J. Apell, M. Roudna, R.A. Schwendener, H.G. Weder and P. Läuger, Biochim. Biophys. Acta 854 (1986) 270.
13 G. Hall and J.M. Watt, Modern numerical methods for ordinary differential equations (Clarendon, Oxford, 1976).
14 J.R. Brocklehurst, R.B. Freedman, D.J. Hancock and G.K. Radda, Biochem. J. 116 (1970) 721.
15 E.A. Haigh, K.R. Thulborn, L.W. Nichol and W.H. Sawyer, Aust. J. Biol. Sci. 31 (1978) 447.
16 E. Blatt, R.C. Chatelier and W.H. Sawyer, Chem. Phys. Lett. 108 (1984) 397.
17 C. Tanford, Physical chemistry of macromolecules (Wiley, New York, 1961) p. 533.
18 S. McLaughlin and H. Harary, Biochemistry 15 (1976) 1941.
19 C.L. Bashford, B. Chance, J.C. Smith and T. Yoshida, Biophys. J. 25 (1979) 63.
20 G. Scatchard, Ann. N.Y. Acad. Sci. 51 (1949) 660.
21 R.J. Clarke and H.-J. Apell, in: Structure, dynamics and equilibrium properties of colloidal systems, ed. E. Wyn-Jones (NATO Advanced Study Institute Series, Kluwer, Dordrecht, 1990) in the press.
22 B. Ketterer, B. Neumcke and P. Läuger, J. Membrane Biol. 5 (1971) 225.
23 V.S. Markin, P.A. Grigorev and L.N. Yermishkin, Biofizika 16 (1971) 1011.
24 O.S. Andersen, S. Feldberg, H. Nakadomari, S. Levy and S. McLaughlin, Biophys. J. 21 (1978) 35.
25 H.-J. Apell and B. Bersch, Biochim Biophys. Acta 903 (1987) 480.
26 G. Cabrini and A.S. Verkman, J. Membrane Biol. 92 (1986) 171.
27 J.R. Bunting, T. Phan, E. Kamali and R.M. Dowben, Biophys. J. 56 (1989) 979.
28 J.C. Smith, P. Russ, B.S. Cooperman and B. Chance, Biochemistry 15 (1976) 5094.
29 G. Adam, P. Läuger and G. Stark, Physikalische chemie und biophysik, 2nd edn (Springer, Heidelberg, 1988) p. 414.
30 J.D. Jackson, Classical electrodynamics (Wiley, New York, 1962) p. 9, 619.
31 R.J. Clarke, H.-J. Apell and P. Läuger, Biochim. Biophys. Acta 981 (1989) 326.
32 G. Stark and R. Benz, J. Membrane Biol 5 (1971) 133.
33 G. Stark, R. Benz and P. Läuger, in: Biomembranes–lipids, proteins and receptors, eds R. M. Burton and L. Packer (BI–Science Publications Division, Webster Groves, MO, 1975) p. 145.